

Mathematical Analysis carried out on the Study of Compatibility, De-lamination and Load-bearing Capacity of Synthetic Diamond Coatings Deposited on Tungsten Carbide Composites

Kaleem Ahmad Najar^{1*}, N. A. Sheikh¹, M. Mursaleen Butt¹, M. A. Shah²

¹Department of Mechanical Engineering, National Institute of Technology Srinagar 190006, India.

²Department of Nano-science, National Institute of Technology Srinagar 190006, India.

*Corresponding author: Kaleem Ahmad Najar, Department of Mechanical Engineering, National Institute of Technology Srinagar 190006, India; E-mail: najar.kaleem@gmail.com

Abstract

Experiments were conducted here for the fabrication of thin films of Nano Crystalline Diamond (NCD) and Micro Crystalline Diamond (MCD) on tungsten carbide composite (WC-6%Co) materials using Hot Filament Chemical Vapor Deposition (HFCVD) method, under pre-determined process parameters. The crystalline quality, microstructure, compositional analysis and grain size of these synthetic diamond coatings were compared using X-ray diffraction (XRD), Raman spectroscopy and Scanning Electron Microscopy (SEM) techniques. The general parameters affecting the integrity of NCD and MCD coatings on WC-6%Co substrates were studied and mathematical analysis was carried out for calculating the force of de-lamination and load-bearing capacity of these coatings. Thus, a comparison has been documented between two fundamental types of synthetic diamond coatings for the purpose of specifying their significance during Machining and Tribological applications.

Keywords: Nano-microcrystalline; Surface Morphology; Structural Characterization; Interfacial Integrity; De-lamination; Load-bearing Capacity.

Introduction

Synthetic diamond coatings have shown excellent mechanical and Tribological properties (such as high hardness, good wear resistance and a low friction coefficient) when sliding against many ceramic counter bodies. Commonly, these synthetic diamond films are obtained through CVD technique using initial process parameters^[1,2].

Fundamentally, on the basis of grain size diamond films fabricated through CVD process has been classified as MCD and NCD. NCD coatings show generally nanocrystallinity comparable to the coating thicknesses of $\sim 3\mu\text{m}$. The average grain size and surface roughness of NCD coating increase with the increase in thickness^[3]. NCD films are especially suitable for Tribological applications and are obtained by minimizing the grain size to the dimension of nanometers, but the internal thermal residual stresses within a coating can be increased with the decrease in grain size^[4]. Due to the presence of high amount of sp²-carbon content, NCD films have shown less adhesion quality on ceramic substrates in comparison to crystallized MCD films and this shows that the force of adhesion will be higher if there is minimum percentage of graphitic-carbon phase at the interface of coating and substrate^[5]. The crystalline quality and mechanical properties of the NCD films will be highly affected due to the presence of larger number of grain boundaries, which contain high amount of graphitic-carbon^[6]. In synthetic diamond growth the columnar grain structure is always observed and is an important parameter to identify the morphology of thick films^[7]. The adhesive quality of diamond coatings is also significantly influenced by the film microstructure. Thus, the surface roughness (impurity), surface morphology and microstructure of a coating are the important

Received date: April 4, 2019

Accepted date: April 15, 2019

Published date: April 17, 2019

Citation: Kaleem Ahmad Najar, et al. Mathematical Analysis carried out on the Study of Compatibility, De-lamination and Load-bearing Capacity of Synthetic Diamond Coatings Deposited on Tungsten Carbide Composites. (2019) J Nanotechnol Material Sci 6(1): 10-16.

Copyright: © 2019 Kaleem Ahmad Najar. This is an Open access article distributed under the terms of Creative Commons Attribution 4.0 International License.

factors for improving the adhesion quality of diamond film on the substrate^[8,9]. Many quantitative and qualitative experimental techniques can be used to analyze the adhesion characteristics of the coatings like, dynamic scratch adhesion test and indentation test^[10,11]. The Raman line-width is linearly related to both the film growth rate and inverse of the grain size, measured by X-ray method. Thus, the grain size of the coating is also linearly related to the inverse of film growth rate^[12].

Two components of residual stresses are developed in diamond films; one is internal stress and the other is thermal stress (produced due to the difference in thermal expansion coefficients between substrate and coating). Thus, the residual thermal stresses are mostly affecting the adhesion strength of diamond films on the substrate^[13]. The grain size of diamond coating can be increased from nanometers to micrometers with the increase in coating thickness and this will also increase the internal residual stresses. Also, increasing the coating thickness improves the resistance of coating de-lamination and load-bearing capacity^[14]. Generally, the force of adhesion between coating and substrate can be improved by increasing the contact area^[15]. For a large area diamond coated flat substrate the thermal strain produced in the film can be calculated from Equation (1), neglecting strain at the edges. Also, under plane strain conditions the resulting thermal stresses can be calculated from Equation (2)^[16].

$$\epsilon_{th} = \sum_{T_s}^{T_s} [\alpha_s - \alpha_D] \Delta T \dots\dots\dots (1)$$

$$\sigma_{th} = \frac{E_D \times \epsilon_{th}}{(1 - \nu_D)} \dots\dots\dots (2)$$

Where, α_s and α_D are the thermal expansion coefficients of the substrate and coating, respectively, T_s is the growth temperature of coating and T_R is room temperature. E_D is the elastic modulus of coating and ν_D is its Poisson's ratio.

In this research, each NCD and MCD coating were deposited experimentally on chemically etched WC-6%Co substrates after maintaining the optimum process parameters. The surface characteristics, like crystalline quality and microstructure of the NCD and MCD coatings were characterized using XRD, Raman and SEM techniques. Especially, the parameters affecting the integrity of coating and substrate system were stud-

ied and mathematical analysis were carried out for calculating the force of de-lamination and load-bearing capacity of NCD and MCD coatings.

Materials and Methods

Cemented tungsten carbide (Cerazitit-CTF12A, with 6% Co and 0.8–1.3 μ m WC grain size) was selected as the substrate material. Samples with dimensions 1cm \times 1cm \times 0.3cm were cleaned in ethyl alcohol with ultrasonic agitation to remove the surface impurities from the substrate. Since, on the surface of WC-6%Co substrate the presence of cobalt opposes the growth of diamond films as it promotes the formation of graphitic-carbon, which decreases the adhesion quality of the diamond coatings. Hence, before the deposition of high-quality diamond films on carbide-substrates the chemical etching is a very important step. The whole steps of surface pre-treatment procedure for WC-6%Co substrates are listed in Table1.

The HFCVD is a widely used deposition technique to achieve different kinds of synthetic diamond coatings on carbides and ceramics for their industrial applications. The mechanical and Tribological properties of diamond coatings are mainly influenced by their grain size and crystalline quality. These crystallinity and grain size of the diamond films are very important factors which are mostly controlled by methane percentage (%CH₄/H₂) ratio and chamber pressure. For the growth of crystalline diamond, the methane concentration can be varied from 1% – 5% and the chamber pressure can be varied from 5–55 Torr, using initial pre-programmed recipe. The other parameters which influence the crystalline quality and the growth rate of the diamond coatings are substrate temperature (700 – 900°C), filament temperature (1800 – 2200°C) and filament to substrate distance (10 – 40mm).

In this work, HFCVD system (Model 650 series, sp³ Diamond Technologies) with improved process control capabilities was used for the deposition of synthetic diamond films. During deposition process, chamber pressure and methane concentration were controlled automatically by using throttle valve and mass flow controllers, respectively. In every experiment, an array of tungsten wires (ϕ 0.12 mm) were used as hot filaments for the activation of precursor gases (H₂ and CH₄) and the con-

Table 1: Surface pre-treatment details for the growth of MCD & NCD coatings

| S. No. | Procedural details | Chemicals | Remarks |
|--------|---|---|--------------------------|
| 1 | Clean Substrate in Soap Solution | Detergent Powder | Ultrasonic Agitation |
| 2 | Rinse Substrate in Distilled Water | - | Dry with hot air |
| 3 | Degrease Substrate | Acetone | Ultrasonic Agitation |
| 4 | Rinse Substrate in Distilled Water | - | Dry with hot air |
| 5 | WC Etching for 10 minutes, Murakami's Reagent | Potassium Hydroxide, Potassium Ferricyanide | Ultrasonic Agitation |
| 6 | Rinse Substrate in Distilled Water | - | Dry with hot air |
| 7 | Cobalt etching for 10 seconds using Caro's acid | Sulfuric Acid (H ₂ SO ₄), Hydrogen Peroxide (H ₂ O ₂) | Highly reactive solution |
| 8 | Rinse Substrate in Distilled Water | - | Dry with hot air |
| 9 | Ultrasonic Cleaning for 2 minutes | Ethanol | Ultrasonic Agitation |
| 10 | Diamond Seeding for 10 minutes | Diamond Seeds Dispersed in Dimethyl Sulfoxide (DMSO) | Ultrasonic Agitation |
| 11 | Rinse and Clean for 2 minutes | Isopropanol | Ultrasonic Agitation |
| 12 | Dry with hot air | - | Load samples to chamber |

Table 2: Growth parameters used for the deposition of NCD and MCD films

| Coating Type | Process Pressure (Torr) | CH ₄ /H ₂ ratio (%) | Filament Temperature (°C) | Substrate Temperature (°C) | Duration (hrs.) | Coating Thickness |
|--------------|-------------------------|---|---------------------------|----------------------------|-----------------|-------------------|
| MCD | 36 | 2 | ~2200 | ~850 | 3 | ~3µm |
| NCD | 12 | 4 | ~2200 | ~850 | 3 | ~3µm |

stant filament to substrate distance of 15 mm was maintained. Thus, the growth parameters adopted in this experimental work for the deposition of MCD and NCD coatings are mentioned in Table 2. After the deposition process the toxic exhaust gases produced in the HFCVD chamber were diluted with nitrogen gas, which was used before and after the diamond growth process to flush the chamber. The temperature of the CVD chamber was maintained at ~50°C using a circulating water chiller and was made of aluminum with cooling channels.

Results and Discussions

Physical Characterizations Techniques: The surface topography and microstructure of the NCD and MCD coatings were studied using High Resolution Scanning Electron Microscope (HRSEM, Quanta 3D, FEI). Coating crystallinity was studied using grazing incidence X-ray diffraction (XRD, PANalytical) technique with CuKα (λ=0.154 nm) radiation at 3° grazing angle. Raman microscope (Alpha 300, WITec) with a 488 nm wavelength of laser light was used for the study of structural characterization and also used to study stress state analysis. Generally, for the structural characterization of 3-D polycrystalline bulk or 2-D thin diamond films, X-ray Diffraction (XRD) technique is used to identify the phase purity, types of phases and crystallographic structure of the sample. The analysis revealed the high phase purity, well oriented crystalline and columnar growth of both types of coatings.

The XRD patterns of MCD and NCD coatings are shown in Figure 1 (a, b), respectively. Sharp and strong peaks of cubic diamond coating were observed at the diffraction angles of approximately 44° and 75.5° corresponding to (111) crystal and (220) crystal planes, respectively for both these coatings, along with the substrate (WC) peaks. These peaks confirm the crystallinity of each diamond coating^[17]. It is clearly confirmed that the grain size of MCD coating is found more than NCD coating and also the grain size of carbide material is found more than each diamond coatings, due to the differences in their peak highest. The crystalline quality and chemical nature of the diamond coatings were studied by using Raman spectroscopy technique. Thus, for the confirmation of diamond nature the crystalline diamond coating shows a fundamental stress-free Raman peak around 1332 cm⁻¹^[18]. Figure 2 (a,b) show the Raman spectra of MCD and NCD diamond coatings, respectively. Here there is a shift towards higher side of the first order fundamental Raman peak which is centred at 1333 cm⁻¹, is indicative of the presence of residual compressive stresses in both these coatings. Mostly, due to the difference in thermal expansion coefficients between the substrate and coating these compressive residual stresses are produced^[19]. Residual stresses can be calculated easily from the equation $\sigma = -0.348 (v_m - v_0)$ GPa for the un-split Raman peak at v_m , where $v_m = 1333$ cm⁻¹ and $v_0 = 1332$ cm⁻¹. Thus, each deposited diamond film accommodates the compressive stresses of

0.348GPa^[20]. The other two peaks observed at $v_1 = 1143$ cm⁻¹ and $v_3 = 1431$ cm⁻¹, represent the characteristics of in-plane (C–H) and stretching (C=C) vibrational modes, respectively. The presence of transpoyacetylene (TPA) chain in the grain boundaries of NCD coatings is the main source of these modes^[21]. Also, the quality factor (Q) was calculated for the deposited diamond films by using the following formula^[22].

$$Q = \left\{ \frac{I_d}{I_{d+I_{glc}}} \right\} \times 100\% \dots \dots \dots (3)$$

Where, I_d is the intensity of the sharp diamond peak and I_{glc} is the intensity of the graphitic-carbon broad peak. From Equation (3), for NCD coating; $Q = \left\{ \frac{1333 \text{ cm}^{-1}}{1333 \text{ cm}^{-1} + 1546 \text{ cm}^{-1}} \right\} \times 100\% = 46\%$

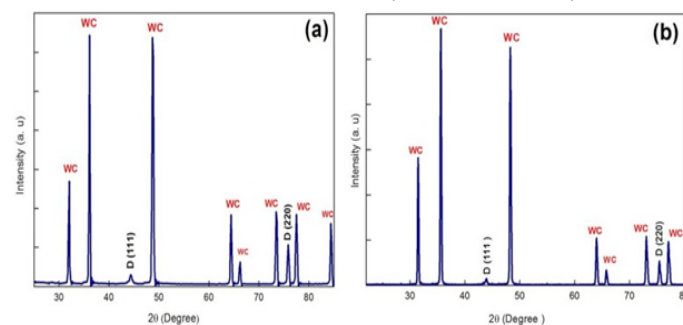


Figure 1: X-ray diffraction patterns of (a) MCD and (b) NCD coatings

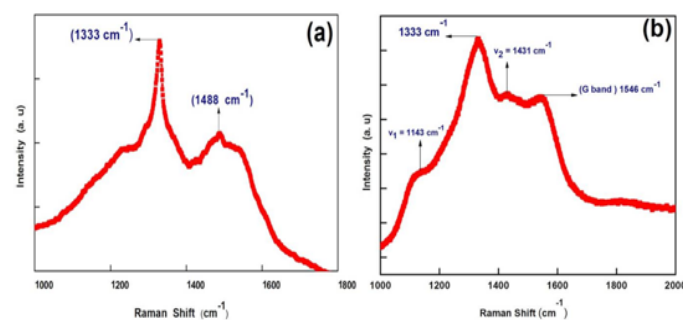


Figure 2: Raman Spectra of (a) MCD coating and (b) NCD coating

The surface morphology, microstructure and grain size of the diamond films were studied by HRSEM technique. Figure 3 (a, b, c) show the SEM images of NCD coating at different magnifications, with grain size lying in the range of 0.2–0.6µm on its surface morphology. In this aspect, the average grain size is calculated from the histogram of its SEM image as ~0.35µm, shown in Figure 3(d). When the concentration of methane is increased from 2–4%, the formation of secondary nucleation starts and retards the growth of the existing grains, thus a cauliflower type of grain structure is commonly observed on NCD surface. Nano-features with normal grain growth were observed all over the surface and these are the important characteristics of thin nanocrystalline diamond coatings^[3]. Generally, on the surface of MCD film the columnar structure of grains and faceted form

of surface morphology were observed. Similarly, Figure 4 (a,b, c) show the SEM images of MCD coating at different magnifications, with grain size lying in the range of 0.3–0.8 μm on its surface. In this aspect, the average grain size is calculated from the histogram of its SEM image as $\sim 0.57\mu\text{m}$, shown in Figure 4 (d).

For the purpose of comparison, the general characteristics of WC–Co, MCD and NCD are summarized in Table 3. Figure 5 (a,b) show the typical cross-sectional morphologies of the NCD and MCD coatings respectively, along with the thickness of both coating and substrate. The compositional analysis on the surfaces of both coatings was confirmed using energy dispersive spectroscopy (EDS) technique, as shown in Figure 6.

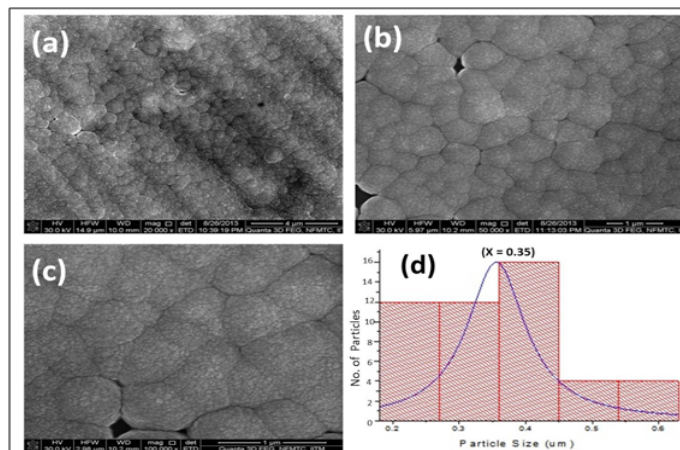


Figure 3 (a, b, c): SEM images of NCD coating at different magnifications and (d) Histogram of the SEM image

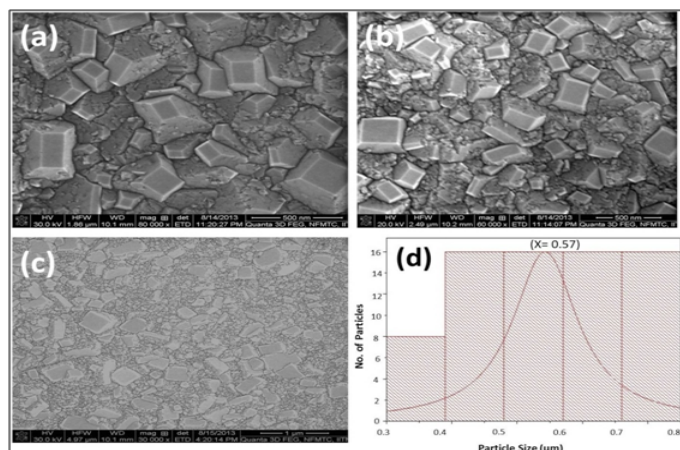


Figure 4 (a, b, c): SEM images of MCD coating at different magnifications and (d) Histogram of the SEM image

Table 3: General Characteristics of WC–Co, NCD and MCD

| Material Type | Average Surface Roughness Factor (R_a) | Average Grain Size (X) | Surface Area | Residual Thermal Compressive Stresses (σ) | Thickness (t) | Elastic Modulus (E) |
|---------------|--|------------------------|---|--|---------------------|-----------------------|
| WC–Co | $\sim 0.35\mu\text{m}$ | $\sim 1.05\mu\text{m}$ | $1\text{cm} \times 1\text{cm} = 1\text{cm}^2$ | $0.348\text{GPa} = 34800 \text{ N/cm}^2$ | 0.3cm | $\sim 550\text{GPa}$ |
| NCD | $\sim 0.19\mu\text{m}$ | $\sim 0.35\mu\text{m}$ | | | $\sim 3\mu\text{m}$ | $\sim 1000\text{GPa}$ |
| MCD | $\sim 0.28\mu\text{m}$ | $\sim 0.57\mu\text{m}$ | | | $\sim 3\mu\text{m}$ | $\sim 1100\text{GPa}$ |

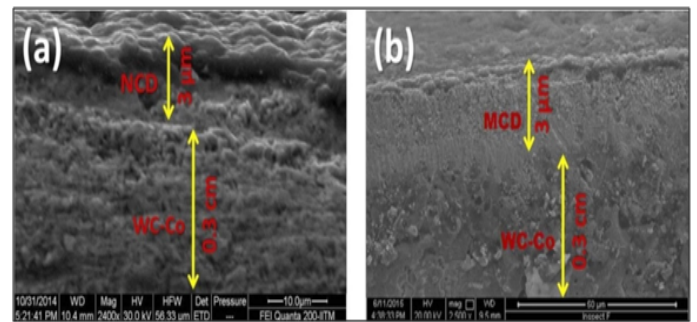


Figure 5: Cross-sectional morphologies of (a) WC–Co/NCD and (b) WC–Co/MCD coating-substrate systems

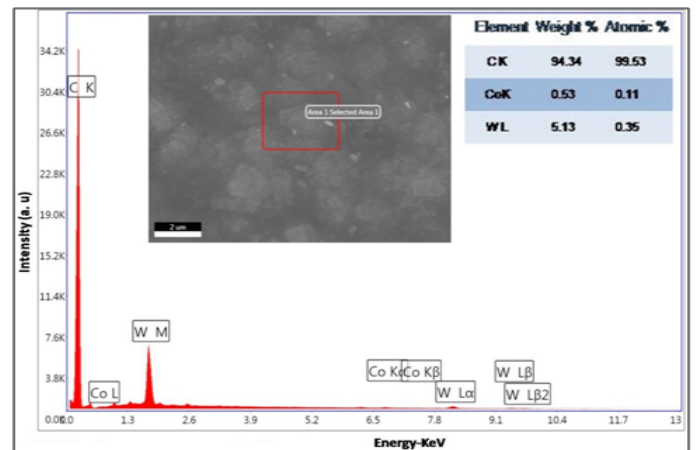


Figure 6: Energy dispersive spectroscopy analysis (EDS) on the surfaces of NCD and MCD coatings

Nano-indentation and Hardness Measurement: Before Nano-indentation testing the NCD and MCD coatings was polished using a Tribometer and sliding against Si_3N_4 pin for the duration of 2hrs. For these polished NCD and MCD coatings, Figure 7 (a, b) show their load-displacement curves, respectively. Thus, four indentation tests were carried out on each coating using Berkovich Nano-indenter. The average indentation depths for NCD and MCD coatings were found as $\sim 79.75 \text{ nm}$ and $\sim 74.75 \text{ nm}$ and their excellent average hardness values were in the range of $\sim 37\text{--}40\text{GPa}$ and $\sim 47\text{--}50\text{GPa}$, respectively. Also, the elastic modulus values of NCD and MCD coatings were found as $\sim 1000\text{GPa}$ and $\sim 1100\text{GPa}$ respectively, as calculated from the Oliver and Pharr mathematical method^[23].

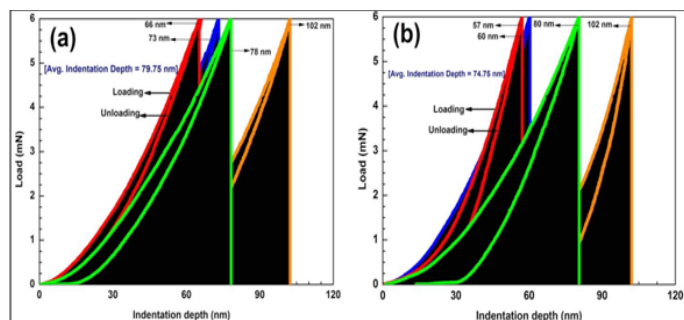


Figure 7: Load-displacement curves corresponding to 4 indentations on (a) NCD and (b) MCD coatings

Parameters Affecting the Adhesion Characteristics of MCD and NCD Coatings: The parameters on which the strength of adhesiveness between coating and substrate system mainly depends are:

- (1) Surface roughness of substrate before deposition
- (2) Elastic modulus of substrate
- (3) Contact surface area between coating and substrate
- (4) Coating thickness
- (5) Grain size of coating and
- (6) Compressive thermal stresses at the interface of coating-substrate system.

Compressive thermal stresses (σ) cannot be eliminated, as they were produced during the deposition and cooling down process of coatings in HFCVD. These stresses mainly depend on temperature of substrate during diamond growth, presence of graphitic carbon at grain boundaries and thickness of coating.

Consider a diamond coating of thickness t (μm). Suppose, S (cm^2) be the contact area between substrate and coating and σ ($\text{Newton}/\text{cm}^2$) be the magnitude of compressive residual stresses at the interfaces of coating and substrate. Let X (nm or μm) be the average grain size and N be the number of grain particles (approximately) on the surface of coating, as both can be calculated from the histogram of SEM image. Therefore, total size of all grain particles on the surface of coating is equal to NX .

Force Causing the De-lamination of MCD and NCD Coatings: If F ($\text{Newton}/\text{cm}^3$) represents the force per unit volume, causing de-lamination between coating and substrate system, then it mainly depends on: σ , t , NX and $1/S$. Combining above equations, $F \propto \frac{\sigma \times t \times (NX)}{S}$ and suppose, $NX = A$, then $F \propto \frac{\sigma \times t \times A}{S}$

$$\text{Or } F = k [(\sigma \times t \times A) / S] \dots\dots\dots (4)$$

Where k is a constant of proportionality and it depends inversely on the roughness factor, Ra (μm or nm) of WC-Co surface before deposition i.e. $k \propto \frac{1}{Ra}$. Since the strength of adhesion between coating and substrate increases with increase in the value of Ra , therefore the force of de-lamination decreases with the increase in value of Ra . This clearly suggests that why chemical etching is necessary for the surface of WC-Co substrate before diamond deposition. During chemical etching the surface roughness has been increased and more cavities were produced in order to increase the adhesion of coating on substrate.

From Equation (4),

$$F = \frac{1}{Ra} \left[\frac{\sigma \times t \times A}{S} \right] \dots\dots\dots (5)$$

Or

$$F \left(\frac{\text{Newton}}{\text{cm}^3} \right) = \frac{1}{Ra(\mu\text{m})} \left[\frac{\sigma \left(\frac{\text{Newton}}{\text{cm}^2} \right) \times t(\mu\text{m}) \times A(\mu\text{m})}{S(\text{cm}^2)} \right] \times [10^{-4}] \dots\dots\dots (6)$$

The Equation (6) shows that ‘ F ’ mainly depends on Ra , t , S and A , which describes that the strength of adhesion between coating and substrate can be only improved by increasing the values of Ra and S or by decreasing values of A and t .

Thus, the force of de-lamination, F can be decreased by decreasing the grain size of diamond film, which can be maintained by changing the process parameters during HFCVD process. This equation clearly suggests that nanocrystalline diamond layer has good integrity with WC-Co substrate than microcrystalline diamond layer because of smaller grain size, but presence of graphitic carbon at grain boundaries decreases adhesive force. Also, using thick NCD ($>3\mu\text{m}$) coating decreases its adhesive strength with WC-Co substrate, because increasing thickness increases the grain size.

Calculation of Force of De-lamination for WC-Co/NCD System:

Using Eq. (6),

$$F \left(\frac{\text{Newton}}{\text{cm}^3} \right) = \frac{1}{Ra} \left[\frac{\sigma \left(\frac{\text{Newton}}{\text{cm}^2} \right) \times t(\mu\text{m}) \times A(\mu\text{m})}{S(\text{cm}^2)} \right] \times [10^{-4}]$$

$$= \frac{1}{0.35(\mu\text{m})} \left[\frac{34800 \left(\frac{\text{Newton}}{\text{cm}^2} \right) \times 3(\mu\text{m}) \times \{16 \times 0.35(\mu\text{m})\}}{l(\text{cm}^2)} \right] \times [10^{-4}] = 167.0400, \text{ where for NCD}$$

surface, $A = NX = 16 \times 0.35(\mu\text{m})$.

Calculation of Force of De-lamination for WC-Co/MCD System:

Similarly, $F \left(\frac{\text{Newton}}{\text{cm}^3} \right) = \frac{1}{Ra} \left[\frac{\sigma \left(\frac{\text{Newton}}{\text{cm}^2} \right) \times t(\mu\text{m}) \times A(\mu\text{m})}{S(\text{cm}^2)} \right] \times [10^{-4}]$

$$= \frac{1}{0.35(\mu\text{m})} \left[\frac{34800 \left(\frac{\text{Newton}}{\text{cm}^2} \right) \times 3(\mu\text{m}) \times \{16 \times 0.57(\mu\text{m})\}}{l(\text{cm}^2)} \right] \times [10^{-4}] = 300.1782, \text{ where for MCD}$$

surface, $A = NX = 16 \times 0.57(\mu\text{m})$.

Hence, based on the above calculations, the strength of adhesion for MCD coating is found more than NCD coating on WC-6%Co substrate due to high force of de-lamination required per unit volume for WC-Co/MCD system. This analysis is in accordance with the literature; that NCD coatings have shown less adhesion on ceramic substrates than MCD coatings due to presence of graphitic-carbon phases at their grain boundaries^[5]. Thus, Equation(6) is validated according to literature and can be applied on both diamond coated carbide materials and ceramic materials.

Expression for Load-bearing Capacity: For practical applications, the design of coating-substrate system can be distinguished into three components such as; coating, interface and substrate. The coating should have high wear-resistance, high hardness, low friction coefficient, good surface finish, high oxidation resistance, high fracture toughness, high thermal conductivity and

enough thickness for load-bearing applications. The Interface should have good adhesion and shear strength. The substrate should have high elastic modulus for load-bearing applications, high temperature strength and high thermal conductivity^[24].

Thus, the load-bearing capacity per unit length for the design of coating-substrate system mainly depends on:

- (1) Elastic modulus of substrate
- (2) Coating thickness
- (3) Grain size of coating.

Let E_s (Newton/cm²) = the elastic modulus of substrate and for WC-Co, $E_s = 550$ GPa. If F (Newton) per unit length, be the amount of load-bearing capacity for the design of coating-substrate system, it mainly depends on: E_s , t and A . Combining above equations, $F \propto E_s \times t \times A$.

$$\text{Or } F = Z \times E_s \times t \times A \dots\dots\dots (7)$$

Where, Z (mm) is the property of coating-substrate system, called adhesive critical failure region and can be calculated experimentally during scratch adhesion testing. By simple microscopic analysis the adhesive critical failure regions can be identified and it was found that the NCD and MCD coatings were failed at a scratch distance of about 0.75 mm and 1.57 mm, i.e. $Z_{\text{NCD}} = 0.75$ mm & $Z_{\text{MCD}} = 1.57$ mm^[17].

From Equation (7),

$$F \text{ (Newton)} = Z \text{ (mm)} \times E_s \text{ (Newton/cm}^2\text{)} \times t \text{ (}\mu\text{m)} \times A \text{ (}\mu\text{m)}.$$

$$\text{Or } F \text{ (Newton/cm)} = Z \times E_s \times t \times A \times [10^{-9}] \dots\dots\dots (8)$$

Thus, the above equation clearly shows that, using thick NCD or MCD coating on WC-Co substrate increases its load-bearing capacity.

Calculation of Load-bearing Capacity for WC-Co/NCD System:

Using eq. (8),

$$F \text{ (Newton/cm)} = Z_{\text{NCD}} \text{ (mm)} \times E_s \text{ (Newton/cm}^2\text{)} \times t \text{ (}\mu\text{m)} \times A \text{ (}\mu\text{m)} \times [10^{-9}]$$

$$= 0.75 \text{ (mm)} \times \{550 \times 10^5 \text{ (Newton/cm}^2\text{)}\} \times 3 \text{ (}\mu\text{m)} \times \{16 \times 0.35 \text{ (}\mu\text{m)}\} \times [10^{-9}] = 6930 \times 10^{-4} = 0.6930.$$

Calculation of Load-bearing Capacity for WC-Co/MCD System:

Similarly,

$$F \text{ (Newton/cm)} = Z_{\text{MCD}} \text{ (mm)} \times E_s \text{ (Newton/cm}^2\text{)} \times t \text{ (}\mu\text{m)} \times A \text{ (}\mu\text{m)} \times [10^{-9}]$$

$$= 1.57 \text{ (mm)} \times \{550 \times 10^5 \text{ (Newton/cm}^2\text{)}\} \times 3 \text{ (}\mu\text{m)} \times \{16 \times 0.57 \text{ (}\mu\text{m)}\} \times [10^{-9}] = 23625 \times 10^{-4} = 2.3625.$$

Based on the above calculations, the load-bearing capacity per unit length of MCD coating is found more than NCD coating on WC-6%Co substrate, due to its high hardness and

more grain size. Therefore, Equation (8) is validated according to literature^[5] and can be applied on both diamond coated carbide materials and ceramic materials.

Conclusion

The adhesion quality of NCD and MCD coatings on WC-6%Co substrate can be enhanced by maintaining the parameters like coating-thickness, grain-size of coating and surface roughness of substrate before deposition. However, the adhesion strength of MCD coating is found more than NCD coating on WC-6%Co substrate, due to high force of de-lamination between the interfaces of coating and substrate. Moreover, increasing the thickness of each diamond coating increases only load-bearing capacity of carbide material and thus, the load-bearing capacity of MCD coatings are found more than NCD coatings.

Hence, using smooth synthetic diamond coatings (Single layered, dual layered or multilayered) with optimum thickness, low friction coefficient, high hardness and good interfacial integrity will certainly be applicable in many mechanical industries.

Acknowledgments

The Authors would like to thank MSRC lab (IIT Madras) for the deposition of coatings and Surface Engineering Division (NAL, Bangalore, India) for carrying out indentation tests and Department of Mechanical Engineering, National Institute of Technology Srinagar, J&K, India for their assistance.

References

1. Erdemir, A., Fenske, G., Krauss, A., et al. Tribological properties of nanocrystalline diamond films. (1999) *Surface and Coatings Technology* 120: 565–572. [Pubmed](#) | [Crossref](#) | [Others](#)
2. Sharma, N., Kumar, N., Dhara, S., et al., Tribological properties of Ultrananocrystalline diamond film-effect of sliding counter bodies. (2012) *Tribology International* 53: 167–178. [Pubmed](#) | [Crossref](#) | [Others](#)
3. Williams, O. A., Daenen, M., D'Haen, J., et al. Comparison of the growth and properties of ultrananocrystalline diamond and nanocrystalline diamond. (2006) *Diamond and Related Materials* 15(4-8): 654-658. [Pubmed](#) | [Crossref](#) | [Others](#)
4. Schwarzbach, D., Haubner, R., Lux, B. Internal stresses in CVD diamond layers. (1994) *Diamond and Related Materials* 3: 757–764. [Pubmed](#) | [Crossref](#) | [Others](#)
5. Ravikumar, D, Maneesh, C, Kumar, N., et al. Growth and characterization of integrated nano- and microcrystalline dual layer composite diamond coatings on WC-Co substrates. (2013) *Int J Refractory Metals and Hard Materials* 37: 127-133. [Pubmed](#) | [Crossref](#) | [Others](#)
6. Wiora, M., Brühne, K., Flöter, A., et al. Grain size dependent mechanical properties of nanocrystalline diamond films grown by hot-filament CVD. (2009) *Diamond and Related Materials* 18: 927-930. [Pubmed](#) | [Crossref](#) | [Others](#)

7. Trava-Airoldi, V. J., Corat, E. J., Peña, A. F. V., et al. Columnar CVD diamond growth structure on irregular surface substrates. (1995) *Diamond and Related Materials* 4(11): 1255–1259.
Pubmed | [Crossref](#) | [Others](#)
8. Dauskardt, R. H., Lane, M., Ma, Q., et al. Adhesion and debonding of multi-layer thin film structures. (1998) *Engineering Fracture Mechanics* 61(1): 141–162.
Pubmed | [Crossref](#) | [Others](#)
9. Salgueiredo, E., Almeida, F. A., Amaral, M., et al. A multi-layer approach for enhancing the erosive wear resistance of CVD diamond coatings. (2013) *Wear* 297(1-2): 1064–1073.
Pubmed | [Crossref](#) | [Others](#)
10. Bull, S. J., Berasetegui, E. G. An overview of the potential of quantitative coating adhesion measurement by scratch testing. (2006) *Tribology International*, 39: 99–114.
Pubmed | [Crossref](#) | [Others](#)
11. Buijnsters, J. G., Shankar, P., van Enkevort, W. J. P., et al. Adhesion analysis of polycrystalline diamond films on molybdenum by means of scratch, indentation and sand abrasion testing. (2005) *Thin Solid Films* 474: 186–196.
Pubmed | [Crossref](#) | [Others](#)
12. Ascarelli, P., Cappelli, E., Mattei, G., et al. Relation between the HFCVD diamond growth rate, the line-width of Raman spectrum and the particle size. (1995) *Diamond and Related Materials* 4(4): 464–468.
Pubmed | [Crossref](#) | [Others](#)
13. Woehrl, N., Hirte, T., Posth, O., et al. Investigation of the coefficient of thermal expansion in nanocrystalline diamond films. (2009) *Diamond and Related Materials* 18: 224–228.
Pubmed | [Crossref](#) | [Others](#)
14. Qin, F., Chou, Y. K., Nolen, D., et al. Coating thickness effects on diamond coated cutting tools. (2009) *Surface and Coatings Technology* 204(6-7): 1056–1060.
Pubmed | [Crossref](#) | [Others](#)
15. Saijo, K., Yagi, M., Shibuki, K., et al. Improvements in adhesive strength and cutting performance of diamond-coated tools. (1991) *Surface and Coatings Technology* 47: 646–653.
Pubmed | [Crossref](#) | [Others](#)
16. Sheikh-Ahmad, J., Parikshit, C. Effect of Cutting-Edge Geometry on Thermal Stresses and Failure of Diamond Coated Tools. (2015) *Procedia Manufacturing* 30: 1–12.
Pubmed | [Crossref](#) | [Others](#)
17. Ravi kumar, D., Kumar, N., Kumaran, C. R., et al. Adhesion characteristics of nano- and micro-crystalline diamond coatings: Raman stress mapping of the scratch tracks. (2014) *Diamond and Related Materials* 44: 71–77.
Pubmed | [Crossref](#) | [Others](#)
18. Praver, S., Nemanich, R. J. Raman spectroscopy of diamond and doped diamond. (2004) *Philos Trans A Math Phys Eng Sci* 362(1824): 2537–2565.
[Pubmed](#) | [Crossref](#) | [Others](#)
19. Gunnars, J., Alahelisten, A. Thermal stresses in diamond coatings and their influence on coating wear and failure. (1996) *Surface and Coating Technology* 80(3): 303–312.
Pubmed | [Crossref](#) | [Others](#)
20. Maneesh, C., Kumaran, C. R., Gowthama, S., et al. Chemical vapor deposition of diamond coatings on tungsten carbide (WC–Co) riveting inserts. (2013) *International Journal of Refractory Metals and Hard Materials* 37: 117–120.
[Pubmed](#) | [Crossref](#) | [Others](#)
21. Kuzmany, H., Pfeiffer, R., Salk, N., et al. The mystery of the 1140cm⁻¹ Raman line in nanocrystalline diamond films. (2004) *Carbon* 42: 911–917.
[Pubmed](#) | [Crossref](#) | [Others](#)
22. Ali, N., Neto, V. F., Mei, S., et al. Optimization of the new time-modulated CVD process using the Taguchi method. (2004) *Thin Solid Films* 469–470: 154–160.
[Pubmed](#) | [Crossref](#) | [Others](#)
23. Oliver, W. C., Pharr, G. M. Improved technique for determining hardness and elastic modulus using load and displacement sensing indentation experiments. (1992) *Journal of Materials Research* 7: 1564–1583.
[Pubmed](#) | [Crossref](#) | [Others](#)
24. Rickerby, D. S., Burnett, P. J. The wear and erosion resistance of hard PVD coatings. (1987) *Surface and Coatings Technology* 33: 191–211.
[Pubmed](#) | [Crossref](#) | [Others](#)

Submit your manuscript to Ommega Publishers and we will help you at every step:

- We accept pre-submission inquiries
- Our selector tool helps you to find the most relevant journal
- We provide round the clock customer support
- Convenient online submission
- Thorough peer review
- Inclusion in all major indexing services
- Maximum visibility for your research

Submit your manuscript at



<https://www.ommegaonline.org/submit-manuscript>